

Topographical Imaging of an Intermembrane Junction by Combined Fluorescence Interference and Energy Transfer Microscopies

Amy P. Wong and Jay T. Groves*

Department of Chemistry
University of California
Berkeley, California 94720

Received July 20, 2001

Pattern formation, in both membrane composition and topography, at the junction between two cells is emerging as a critical element of intercellular communication and signal transduction. For example, distinctive patterns of proteins, a synapse, have recently been observed to form in the membranes of living T-cells and NK-cells during recognition of antigen presenting cells.^{1–3} Quantitative analysis of the T-cell synaptic junction suggests that the reaction environment created by the membrane–membrane interface can drive pattern formation by spontaneous processes.⁴ This provides a membrane-based signal amplification mechanism which translates subtle differences in protein binding kinetics into large-scale pattern rearrangements. To investigate the physical principles behind cell membrane organization and cell recognition, we have developed a supported membrane system which models the environment of a cell–cell junction.

An intermembrane junction is created between a supported membrane and an upper membrane patch, which is deposited from a giant vesicle (Figure 1). Incorporation of different fluorescent probe lipids into each of the two membranes enables a variety of fluorescence imaging capabilities which we employ to obtain both lateral and topographical information about the junction. Fluorescence resonance energy transfer (FRET) between the two membranes when they are closely apposed (<4 nm) is shown to leave a footprint, which maps the contact zone. Larger topographical features can be observed by fluorescence interference contrast microscopy⁵ (FICM) when the membrane system is supported on an oxidized silicon wafer. In this configuration, near-field interference effects set up optical standing waves that provide contour mapping of the membrane topography. Several studies have examined membrane–membrane interactions using intact giant vesicles resting on supported membranes.^{6,7} In those investigations, membrane topography was imaged by reflection interference contrast microscopy (RICM), which relies on interference between light reflected from the membrane surface and the inner surface of the transparent substrate. Both RICM and FICM are capable of revealing topographical features with nanometer resolution. However, the use of fluorescence is simple and greatly facilitates distinction of one membrane from another at an intermembrane junction. Here, we demonstrate how two fluorescence techniques, intermembrane FRET and FICM, can be combined into a powerful observation scheme that illuminates both lateral and topographical features of a supported membrane junction on multiple-length scales.

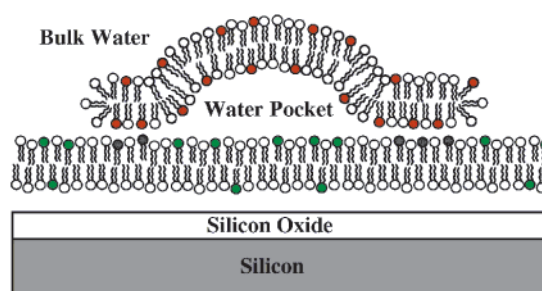


Figure 1. Schematic of the supported membrane junction. The lower membrane is a conventional supported membrane^{8,9} which is trapped ~1 nm above the underlying silicon oxide surface. The upper membrane is deposited by rupture of a single giant vesicle. Although both membranes are laterally fluid, the top membrane is also flexible in the dimension perpendicular to the interface. This allows topographical patterns to form at the membrane junction.

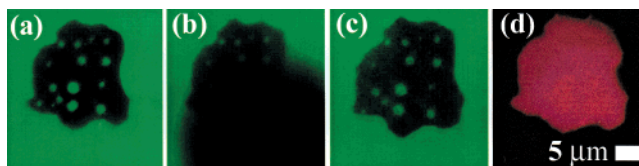


Figure 2. (a) Intermembrane FRET footprint of upper bilayer on the underlying membrane. (b) Photobleached spot in lower membrane. (c) Full recovery of bleached spot by diffusive mixing in 5 min. (d) Image of Texas Red-labeled upper bilayer membrane patch. This experiment was performed on a glass coverslip. In the absence of any interference effects, the upper membrane is seen to be continuous. The upper bilayer contained 6% DODAP, 1% Texas Red DHPE, and 93% DMPC by mole, whereas the supported bilayer is composed of 7% DODAP, 2% NBD-PG, 91% DMPC. The aqueous solution contained 60 mM NaCl.

Intermembrane FRET reveals regions over which the two membranes are in close proximity. Overlap between the emission spectrum of NBD-PG (green), in the lower membrane, and the absorption spectrum of Texas Red DHPE, in the upper membrane, leads to efficient quenching of the NBD fluorescence when the two are separated by less than 4 nm.¹⁰ Figure 2 illustrates adhesion patterns observed by intermembrane FRET. After junction formation between the two membranes, a footprint of the region of close apposition is observed as the darkened area in Figure 2a. Domains of unquenched NBD fluorescence within this region reveal that the intermembrane junction is not uniform. Although the upper membrane is continuous (see the Texas Red fluorescence image in Figure 2d), it is not in continuous contact with the underlying membrane. Sackmann et al. have observed a similar adhesion phenomenon by RICM with a giant vesicle system.^{6,7} Adhesion between membranes doped with oppositely charged lipids can result in the formation of blisters surrounded by regions of tight adhesion. This effect has been attributed to adhesion-induced reorganization of charged lipids within the fluid membranes. In our experiment, an intermembrane junction is formed between mixed membranes, containing both positively and negatively charged lipids, with equivalent net positive charge densities. Thus, metastable adhesion phenomena can occur between like-charged membranes.

Figure 2, b and c, illustrates semiquantitative photobleach recovery experiments performed on the lower membrane. These demonstrate the lateral fluidity of the membrane as well as the connectivity throughout the adhesion zone. Note the fluorescence

(1) Grakoui, A.; Bromley, S. K.; Sumen, C.; Davis, M. M.; Shaw, A. S.; Allen, P. M.; Dustin, M. L. *Science* **1999**, *285*, 221.

(2) Monks, C. R. F.; Freiberg, B. A.; Kupfer, H.; Sciaky, N.; Kupfer, A. *Nature* **1998**, *395*, 82.

(3) Davis, D. M.; Chiu, I.; Fassett, M.; Cohen, G. B.; Mandelboim, O.; Stominger, J. L. *Proc. Natl. Acad. Sci. U.S.A.* **1999**, *96*, 15062.

(4) Qi, S. Y.; Groves, J. T.; Chakraborty, A. *Proc. Natl. Acad. Sci. U.S.A.* **2001**, *98* (12), 6548.

(5) Lambacher, A.; Fromherz, P. *Appl. Phys. A* **1996**, *63*, 207.

(6) Nardi, J.; Bruinsma, R.; Sackmann, E. *Phys. Rev. E* **1998**, *58* (5), 6340.

(7) Kloboucek, A.; Behrisch, A.; Faix, J.; Sackmann, E. *Biophys. J.* **1999**, *77*, 2311.

(8) Groves, J.; Ulman, N.; Boxer, S. *Science* **1997**, *275*, 651.

(9) Sackmann, E. *Science* **1996**, *271*, 43.

(10) Lakowicz, J. *Principles of Fluorescence Spectroscopy*; Kluwer Academic: New York, 1999.

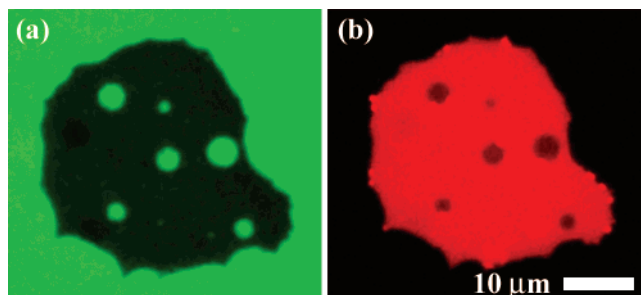


Figure 3. FICM images of lower (a) and upper (b) membranes on a silicon wafer with 100 nm oxide layer. Domains of reduced fluorescence in the upper membrane reveal topographical features (blistering, see Figure 1). Within these domains, the intermembrane separation is too large for FRET, resulting in domains of unquenched fluorescence in the lower membrane. Domains seen in (b) are not visible on transparent substrates (see Figure 2a for comparison). These images were viewed with a 60× long working distance air objective.

recovery of the unquenched domains within the adhesion zone. Similar photobleach experiments on the upper bilayer (See Supporting Information) confirm it is fluid as well.

We make use of near-field interference effects to resolve topographical features in the upper bilayer which lie outside the range observable by intermembrane FRET. For these studies, an identical supported membrane configuration was deposited on an oxidized silicon wafer. The oxide layer is transparent, while the underlying silicon surface serves as a reflector. Interference of incident and reflected optical waves modulates the observed fluorescence intensity, F , as a function of distance from the surface, z :

$$F \propto \sin^2\left(\frac{2\pi(n_w z + n_o z_o)}{\lambda_{ex}}\right) \sin^2\left(\frac{2\pi(n_w z + n_o z_o)}{\lambda_{em}}\right) \quad (1)$$

where z is the height above the oxide surface, and z_o is the oxide thickness.¹¹ n_w and n_o are the indices of refraction for water (1.33) and for the silicon oxide layer (1.46), respectively. The excitation and emission wavelengths, λ_{ex} and λ_{em} , are 560 and 645 nm, respectively, for viewing Texas Red DHPE. Images of the supported membrane junction obtained using this form of FICM reveal topographical domains, appearing as spots of reduced Texas Red fluorescence in the upper membrane, which correspond to the domains of unquenched NBD fluorescence in the lower membrane (Figure 3). Interference fringes within the topographical domains of the upper membrane were distinguishable with higher magnification FICM (Figure 4a). These fringes were used to map the three-dimensional shape of the membrane.

Lateral positions of the distinguishable maxima and minima were located and plotted against the corresponding elevation, as determined from eq 1 (Figure 4b). These measurements trace out a roughly spherical surface reaching a maximum height of 510 nm above the underlying oxide surface. Next, the corresponding interference pattern was calculated for this spherical topographic profile and compared with the measured fluorescence pattern (Figure 4c). The major fringe toward the center of the domain is clear; however, the outermost fringe is largely washed out, appearing as only a shoulder in the fluorescence profile. This is expected, given that the optical transfer function of the imaging

(11) Equation 1 is derived for waves traveling normal to the surface from basic optical principles. See, for example: Born, M. *Principles of Optics*; Pergamon Press: London, 1959.

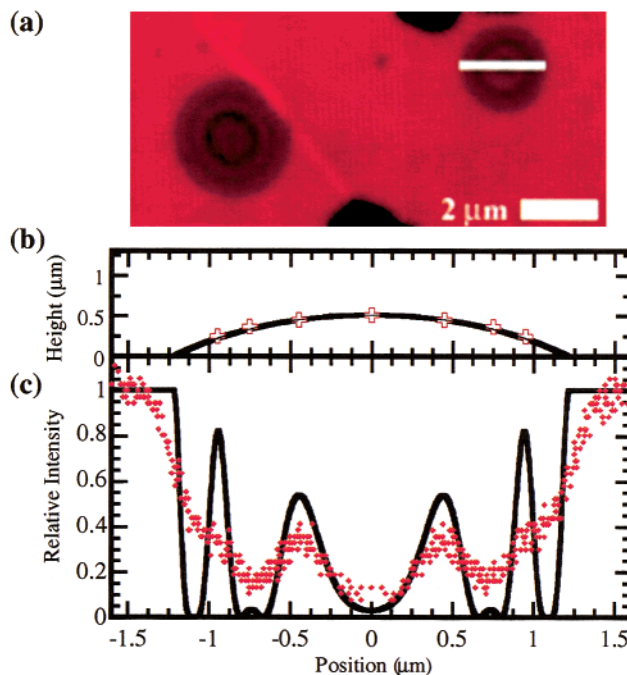


Figure 4. (a) FICM image of the upper membrane using a 100× oil immersion objective with a variable numerical aperture set to ~0.8. White bar in upper right domain marks the source of data analyzed. (b) Plot of lateral positions of interference fringes along the intensity trace against corresponding height above the surface (from eq 1). (c) Measured fluorescence intensity pattern plotted against calculated interference pattern (solid line) for the spherical surface in (b).

system is fundamentally limited by diffraction. Factors not included in eq 1, which may directly compromise the clarity of the fringes, include spectral line widths and membrane fluctuations. More sophisticated image analysis along with the use of multiple-thickness oxide layers can be used to achieve topographical measurements with nanometer resolution.^{5,12}

The supported membrane configuration and combination of fluorescence imaging procedures introduced here significantly facilitate observation of molecular interactions at a membrane–membrane interface. The compositions of both membranes can be controlled independently, and the open configuration allows facile exchange of the aqueous environment. The combination of intermembrane FRET with FICM provides topographical information about the membrane junction on a range of length scales, which spans that of interest for cellular interactions. At the same time, fluorescence imaging of membranes is a highly effective means of examining lateral reorganization processes.¹³ We anticipate that these techniques will prove useful in studies of molecular processes occurring between cell membranes.

Acknowledgment. We gratefully acknowledge financial support from the LDRD program at Lawrence Berkeley National Laboratories and a Burroughs Wellcome Career Award in the Biomedical Sciences (to J.T.G). A.P.W. received support from the Chevron Scholars Research Program.

Supporting Information Available: Fluidity confirmation of the upper bilayer, chemical structures of lipids, information on the deposition of upper bilayer (PDF). This material is available free of charge via the Internet at <http://pubs.acs.org>.

JA016677J

(12) Braun, D.; Fromherz, P. *Phys. Rev. Lett.* **1998**, *81* (23), 5241.

(13) Groves, J.; Boxer, S.; McConnell, H. *Proc. Natl Acad. Sci. USA* **1998**, *95* (3), 935.